COMMUNICATIONS

Magnetic Resonance in Medicine 64:319–326 (2010)

A Simple Low-SAR Technique for Chemical-Shift Selection with High-Field Spin-Echo Imaging

Dimo Ivanov,* Andreas Schäfer, Markus N. Streicher, Robin M. Heidemann, Robert Trampel, and Robert Turner

We have discovered a simple and highly robust method for removal of chemical shift artifact in spin-echo MR images, which simultaneously decreases the radiofrequency power deposition (specific absorption rate). The method is demonstrated in spin-echo echo-planar imaging brain images acquired at 7 T, with complete suppression of scalp fat signal. When excitation and refocusing pulses are sufficiently different in duration, and thus also different in the amplitude of their slice-select gradients, a spatial mismatch is produced between the fat slices excited and refocused, with no overlap. Because no additional radiofrequency pulse is used to suppress fat, the specific absorption rate is significantly reduced compared with conventional approaches. This enables greater volume coverage per unit time, well suited for functional and diffusion studies using spin-echo echo-planar imaging. Moreover, the method can be generally applied to any sequence involving slice-selective excitation and at least one slice-selective refocusing pulse at high magnetic field strengths. The method is more efficient than gradient reversal methods and more robust against inhomogeneities of the static (polarizing) field (B_0). Magn Reson Med 64:319–326, 2010. © 2010 Wiley-Liss, Inc.

Key words: chemical shift; spin-echo; fat suppression; high-field MRI; specific absorption rate; spin-echo echo-planar imaging; fMRI; diffusion imaging

MRI is intended to provide spatially resolved images correctly depicting anatomy. Because MR-visible protons in water and fat have Larmor frequencies that are 3.35 ppm apart, techniques using relatively low receiver bandwidths per voxel suffer from chemical shift artifact, in which the image of fatty tissue can be displaced by several voxels from the water image, with a highly problematic overlap. The magnitude of the displacement depends on magnetic field strength, RF pulse bandwidth, gradient strength, acquisition bandwidth, voxel size, and *k*-space trajectory. This problem can be particularly severe in echo-planar images, where at 7 T the fat artifact can be displaced by 70% of the field of view from the water image. To avoid the chemical shift artifact, other MRI sequences are run with unnecessarily high bandwidths, with a detrimental effect on signal-to-noise ratio.

Department of Neurophysics, Max Planck Institute for Human Cognitive and Brain Sciences, Leipzig, Germany.

*Correspondence to: Dimo Ivanov, M.Sc., Max Planck Institute for Human Cognitive and Brain Sciences, Department of Neurophysics, Stephanstrasse 1a, 04103 Leipzig, Germany. E-mail: divanov@cbs.mpg.de

Received 29 October 2009; revised 28 April 2010; accepted 28 April 2010.

DOI 10.1002/mrm.22518

Published online in Wiley InterScience (www.interscience.wiley.com).

Since the earliest chemical shift imaging publications (1–3) numerous methods have been used to image water and fat tissue distributions separately (4–6). For functional and diffusion-weighted neuroimaging, the fat distribution is usually of little interest. For both applications, single-shot echo-planar imaging (EPI) is often used, because it acquires entire slices in a fraction of a second and thus avoids distributed artifacts associated with head motion. However, EPI acquisitions are sensitive to chemical shift artifacts, which appear in the phase-encoding direction of the acquisition, due to the relatively low bandwidth per voxel compared to the frequency-encoding direction. This is usually mitigated by including a fat-suppression module preceding the (typically) 90° flip angle excitation pulse. The longitudinal relaxation time (T_1) inversion-recovery method, for example, employs an inversion pulse, and the RF excitation pulse is applied when the longitudinal magnetization of the fat protons passes through zero (7). This has the disadvantage of also reducing the water signal. More commonly, a spectrally selective fat-saturation radiofrequency (RF) pulse with a narrow bandwidth is applied, centered on the fat proton frequency (8–10) followed by crusher gradients prior to the main RF excitation pulse. Combination of the two techniques is also possible, known as spectral inversion recovery (11). All such fat-suppression methods require additional RF and gradient pulses, thus increasing the specific absorption rate (SAR) and lengthening the acquisition time. Furthermore, fat saturation pulses generate magnetization transfer contrast, visible in multislice imaging at 3 T (12). Magnetization transfer contrast reduces the remaining water tissue signal, increasing with the number of slices and with shorter repetition times. Increasing the volume coverage per unit time will obviously aggravate the signal loss due to these magnetization transfer contrast effects.

It is evident that methods that do not require additional RF pulses for fat suppression have a distinct advantage. Another approach, the slice-select gradient reversal method, requires no additional pulses, provided that the sequence already contains at least one 180° refocusing pulse (13–15). This method depends on the use of slice-select gradients of opposite polarity for the excitation and refocusing pulses. The idea has recently been demonstrated using two refocusing pulses (16) for imaging water diffusion in the brain at a magnetic field of 3 T.

At higher field strength, the increased SAR and inhomogeneities in the magnitudes of both the static (polarizing) (B_0) and (excitation) RF (B_1) field make effective fat

suppression more difficult. We present a simple and effective method for fat suppression, which is relatively insensitive to B_1 and B_0 field inhomogeneities, and allows substantial reduction of SAR.

THEORY

Our method resembles the gradient reversal technique, in that it uses the fact that the chemical shift of fat manifests itself in the slice-select direction. However, instead of reversing the slice-select gradients during excitation and refocusing, we simply adjust the amplitudes of the gradients to ensure that the excited fat magnetization is dephased rather than refocused, so no observable spin-echo is generated. This is explained as follows.

We assume, without loss of generality, that the MR scanner is set to the water proton resonance frequency. Because of their different chemical environments, the proton spins of water and fat at a given location precess at different frequencies when a gradient is applied. The displacement D (in mm) of the fat slice relative to the water slice for both excitation (D_{exc}) and refocusing (D_{ref}) is given by

$$D = \frac{\delta B_0}{G_s}, \quad [1]$$

where δ is the chemical shift in ppm, B_0 is the main magnetic field in Tesla (T), and G_s is the slice-select gradient strength in mT/m (16). In general, the profiles of the excited and refocused fat slice may differ in thickness, d (mm), so to eliminate overlap, and thus to achieve complete fat-signal suppression, Eq. 2 has to hold:

$$|D_{exc} - D_{ref}| \geq (|d_{exc}| + |d_{ref}|)/2 \quad [2]$$

When the same RF pulse shape is used for excitation and refocusing, the right-hand side of Eq. 2 is replaced by the nominal slice thickness. However, successful fat suppression is independent of specific RF pulse shape, provided that the slice profiles of the fat slice excited and fat slice that should be refocused do not overlap.

Slice-selective RF pulses are characterized by a dimensionless number, the bandwidth–time product, P. As can be seen from Eq. 1, G_s is the key parameter for changing the displacement of both fat slices relative to the water slice, and hence relative to each other. One way of achieving a smaller slice-select gradient strength, while keeping the same slice profile, is to increase the duration of the RF pulse, because

$$\Delta\omega = \gamma d G_s = P/\tau \quad [3]$$

where $\Delta\omega$ is the pulse bandwidth in Hz; d is the slice thickness in mm; γ is the gyromagnetic ratio in MHz/T; and τ is the duration of the RF pulse in s. Lengthening the RF pulse results in a pulse of smaller bandwidth. To achieve the desired slice thickness, the slice-select gradient amplitude is adjusted to match the bandwidth of the pulse. Using Eqs. 1 and 3 in Eq. 2 gives the following expression:

$$\delta B_0 \left| \frac{1}{G_{exc}} - \frac{1}{G_{ref}} \right| \geq \frac{1}{2\gamma} \left(\frac{\Delta\omega_{exc}}{|G_{exc}|} + \frac{\Delta\omega_{ref}}{|G_{ref}|} \right) \quad [4]$$

Furthermore, if the duration of a RF pulse is scaled by a factor c according to expression 5

$$\tau \rightarrow c\tau, \quad [5]$$

and the flip angle, as well as the slice thickness, are kept constant then

$$G_s \rightarrow G_s/c \quad E \rightarrow E/c, \quad [6]$$

where E is the energy deposited by the RF pulse in the sample (17). Therefore, the factor c in expressions 5 and 6 determines both the slice-select gradient and the decrease in power deposition associated with either pulse due to lengthening it.

Equation 7 gives an expression for the difference of the slice-select gradient strengths required for fat suppression. It can be seen that efficient fat suppression can be achieved regardless of which of the two RF pulses is lengthened.

$$|G_{ref} - G_{exc}| \geq \frac{1}{2\delta B_0 \gamma} \left(\frac{P_{exc}|G_{ref}|}{\tau_{exc}} + \frac{P_{ref}|G_{exc}|}{\tau_{ref}} \right) \quad [7]$$

Figure 1 illustrates the proposed method for fat-shift artifact elimination. In Fig. 1a, the excitation of the spins in the object is shown. Because of the chemical shift, the slices of the water spins and the fat spins excited by the RF pulse are displaced by an amount D_{exc} perpendicular to the slice-select direction. If the refocusing pulse has the same bandwidth-time product and duration its slice-select gradient will be the same as those of the excitation pulse and both the excited species will be refocused (see Fig. 1b). Figure 1c illustrates the effect of a refocusing pulse of the same bandwidth-time product as the excitation pulse, but a longer duration. While the RF pulse with the frequency bandwidth $\Delta\omega_{ref}$ refocuses the water protons at the position of the excited water slice, refocusing of fat protons would occur at a position different from the fat slice excited. Essentially, the displacement D_{ref} differs from the excitation displacement D_{exc} because of the smaller slice-select gradient associated with the longer RF pulse. The unrefocused fat signal is further dephased by the slice-selective gradient associated with the refocusing pulse. If the refocusing pulse is surrounded by crusher gradients, a standard precaution for SE EPI as well as for many other spin-echo sequences, the fat signal will be additionally dephased. To refocus the excited fat protons, a long RF pulse with an offset frequency spectrum $\Delta\omega^*_{ref}$ would be necessary.

Equation 8 provides an expression for the duration of the refocussing pulse required to suppress the fat signal, in terms of the excitation pulse duration and the slice-select gradients, irrespective of the sign of the gradients:

$$\tau_{ref} \geq \frac{P_{ref}|G_{exc}|\tau_{exc}}{2\delta B_0 \gamma |G_{ref} - G_{exc}|\tau_{exc} - P_{exc}|G_{ref}|}. \quad [8]$$

The denominator in Eq. 8 needs to be positive as negative pulse durations have no physical meaning. In

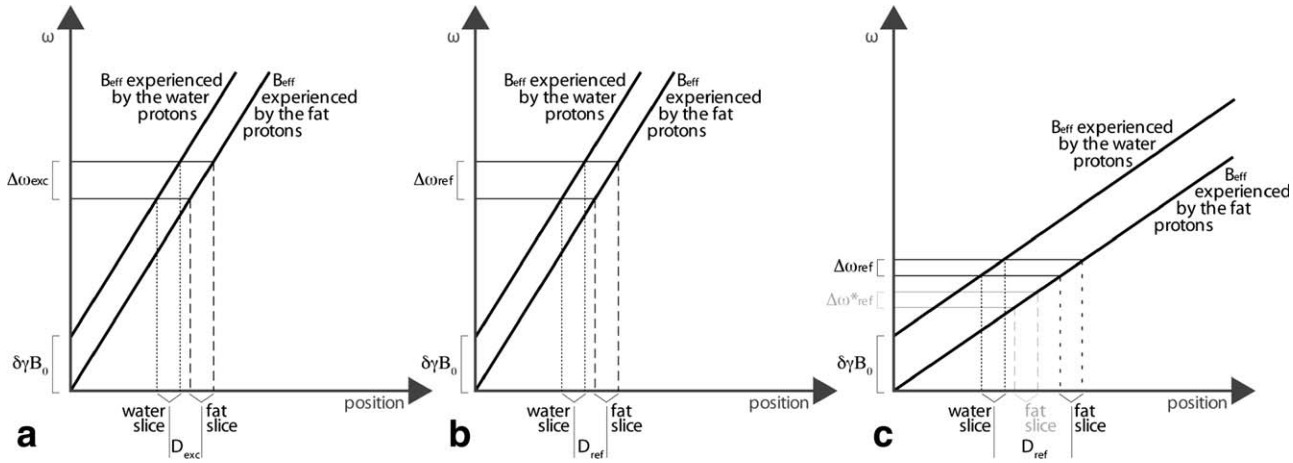

FIG. 1. Illustration of the proposed fat-suppression method. **a**: Excitation of the proton spins in the object by a RF pulse of bandwidth $\Delta\omega_{exc}$. Because of the chemical shift a resonance frequency difference of $\delta\gamma B_0$ exists between the fat and water protons irrespective of the magnetic field gradient G applied. Therefore, the slices of the water spins and the fat spins are displaced by an amount D_{exc} perpendicular to the slice-select direction. **b**: Refocusing with a RF pulse of the same duration and bandwidth-time product as the excitation pulse. The bandwidth and slice-select gradient are the same as during the excitation leading to identical displacement D_{ref} between the fat and water slice refocused. As the signal from both species is refocused, no fat suppression can be obtained. **c**: Refocusing with a RF pulse of longer duration and the same bandwidth-time product as the excitation pulse. The bandwidth and slice-select gradient are smaller than during the excitation leading to larger displacement D_{ref} between the fat and water slice refocused. As only the signal from water is refocused, complete fat suppression is obtained.

particular, the gradient during the refocusing pulse can be equal in magnitude and with opposite sign to the gradient during the excitation pulse. This gives the special case of gradient reversal without variation of the gradient strength (14). The formula for the preferred minimal duration of the excitation pulse can be obtained by exchanging the indices for the refocusing and excitation in Eq. 8.

It is important to note that the main magnetic field strength enters the denominator on the right-hand side of Eq. 8, which means that the proposed method works better at higher fields. At fields lower than 3 T, the RF pulses necessary to achieve complete fat-signal suppression are quite long and slice-select gradients will be quite small, so that practical use in a pulse sequence is provided in exceptional cases only.

Furthermore, for a chosen slice profile and thickness, the shortest possible duration of the refocusing pulse required for fat suppression depends only on the magnitude of the slice-select gradient applied during the excitation pulse, in case the latter has smaller duration. According to Eq. 3, the duration of the excitation pulse decreases with increasing slice-select gradient. The magnitude of the maximum possible gradient is a technical characteristic of the gradient system and will set the lower limit to the duration of the excitation pulse. Another hardware constraint on the shortness of the excitation pulse is the maximum peak voltage that the transmitter RF system can deliver. Necessarily, the duration of the shortest possible excitation pulse determines the duration of the shortest possible refocusing pulse effective for fat suppression. The previous discussion remains true if the excitation pulse and the excitation slice-select gradient are substituted respectively by the refocusing pulse and refocusing slice-select gradient, and vice versa. Although it is advantageous to have both pulses as short as possible, while fulfilling the condition for fat suppression, this can be limited by SAR considerations. An effect that is not considered in the foregoing calculations but is important for very long pulse durations, is the effective transverse relaxation time (T_2*) decay during the RF pulse. While this effect will not degrade the fat suppression achieved, it may affect the overall image quality.

MATERIALS AND METHODS

All experiments were performed on a 7-T whole-body MR scanner (MAGNETOM 7T, Siemens Healthcare Sector, Erlangen, Germany) with a gradient system achieving peak gradient amplitudes of 38 mT/m and a maximum slew rate of 200 mT/(m s), running software version VB 15A. A 24-element phased array head coil (Nova Medical, Wilmington, MA) was used for signal transmission and reception. Two healthy volunteers were included in the study after obtaining their informed consent. Several SE EPI sequences with variable durations of the Siemens product excitation and refocusing pulses were designed and implemented. These pulses are sinc-shaped and Hanning-apodized. The bandwidth-time product was kept constant and chosen to be the same for both pulses (5.22), so that increasing the pulse duration resulted in decreasing its bandwidth, while maintaining the same slice thickness and profile. The flip angle for the excitation pulse was set to 90° and for the refocusing pulse to 180° by the automated scanner routines. The refocusing pulse was surrounded by crusher gradients in all three spatial directions to dephase any residual unrefocused transverse magnetization. Pulse sequences with the following RF pulse combinations were designed and implemented (duration of excitation pulse followed by that of refocusing pulse, in msec): 2.56/2.56, 2.56/3.84, 2.56/6.4, 3.84/2.56, 3.84/3.84, 6.4/2.56, and 6.4/6.4. Figure 2 shows 3 of the used RF pulse combinations with their associated

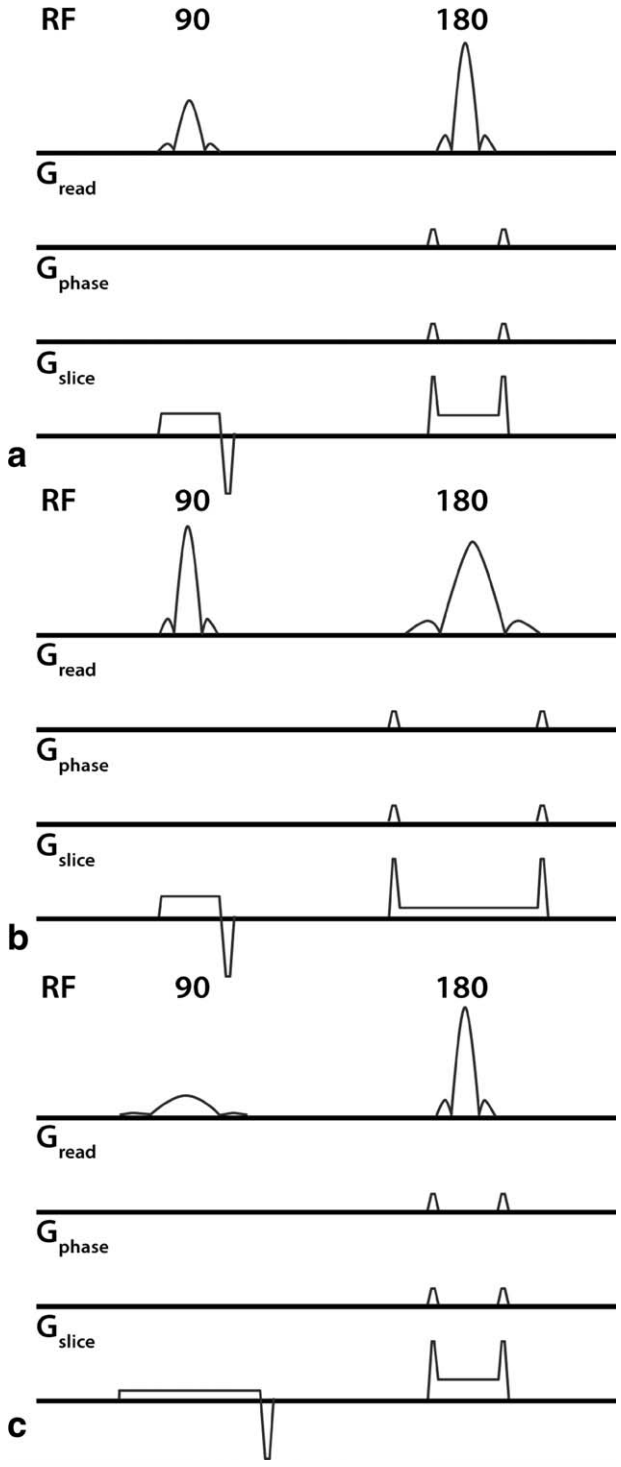

FIG. 2. Spin-echo sequence diagrams of the RF pulses with the respective slice-select and crusher gradients. **a**: 2.56 ms excitation pulse and 2.56 ms refocusing pulse. **b**: 2.56 ms excitation pulse and 6.4 ms refocusing pulse. **c**: 6.4 ms excitation and 2.56 ms refocusing.

gradients. Furthermore, each of these sequences was modified to allow reversal of the slice-select gradient direction during excitation. All of the described variants were executed with 3, 2, and 1 mm slice thickness to examine the effect of increasing magnitude of the slice-select gradients, totaling 42 acquisitions. In addition, every acquisition was done twice with the vendor-provided fat saturation switched on and off. Here, for fat saturation a frequency-selective 5.12 ms Gaussian pulse with a flip angle of 110° and bandwidth of 375 Hz was used, followed by a crusher gradient pulse, which disperses the excited transverse magnetization. The pulse magnitude is more than 90° to counteract the recovery of the fat magnetization in the longitudinal direction, so the implementation can also be considered a variant of the spectral inversion recovery (11). However, as no sequence-timing modification was made to properly take into account the longitudinal relaxation time of fat at 7 T and there are significant flip angle variations throughout the slice due to B_1 inhomogeneities at 7 T, it is justified to consider the result as fat saturation.

A 2D multislice single-shot EPI acquisition without slice gaps was performed with each of the 84 sequence variants described above, in one subject. The shim volume remained the same throughout the experiment. The in-plane resolution was kept relatively low at 3×3 mm^2 to clearly depict remaining fat signal. The imaging matrix was 64 by 64 with field of view 192×192 mm^2. The EPI readout lasted 44 ms, so the bandwidth in the phase-encoding direction was 22.7 Hz. The echo time was set at 55 ms—the smallest possible for the sequence in which both excitation and refocusing pulses had 6.4 ms duration, and equal to the mean T_2 of grey matter at 7 T (18,19). Because a single shot sequence was used with a repetition time of 20 s, any longitudinal relaxation time effects are eliminated. The long TR also allowed whole brain coverage for the scans with 3 and 2 mm slice thickness without exceeding the SAR limit. In the second subject participating in the study 5 image volumes of the same image matrix with TR of 2 s and GRAPPA factor 3 were acquired (20). The SAR limit for the product SE-EPI sequence constrained the number of slices obtainable to 10, which was chosen for the other sequences tested to investigate SAR variation. Parallel imaging was used to shorten the echo-train duration and so minimize distortions and T_2* blurring which can be easily mistaken for drop-outs in susceptibility affected regions. To investigate the sensitivity of the fat suppression methods to B_0 inhomogeneities acquisitions were repeated after the shim was intentionally altered so that the full width at half maximum of the water peak increased from 31 to 115 Hz and that of the fat peak from 310 to 520 Hz.

The individual scans for every slice thickness were coregistered with SPM5 to the first acquired to eliminate effects of inter-scan motion. Then all the scans with 1- and 2-mm slice thickness were coregistered to the 3-mm scans and resampled to 3-mm isotropic resolution. This allowed voxel-wise correspondence between the images to estimate the effect of gradient reversal with increasing slice-select gradients on the water signal. The resulting images were subtracted pair-wise.

RESULTS

The results presented below were obtained with optimally tuned shim unless stated otherwise. Figures 3 and 4 show SE EPI images acquired at the same position in the head at 3 mm isotropic resolution with identical acquisition parameters. In Fig. 3, SE EPI images were acquired with

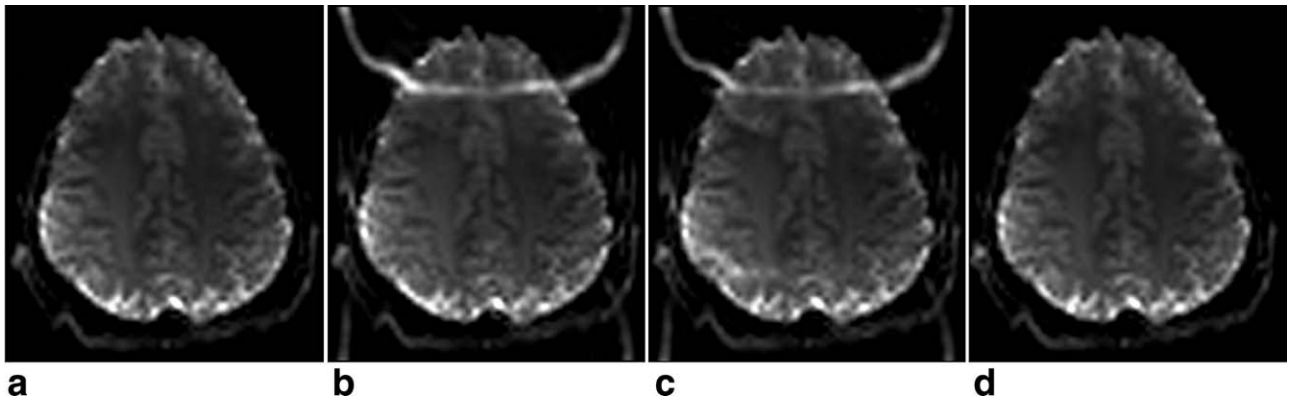

FIG. 3. SE EPI images acquired according to the conventional method with: (**a**) 2.56 ms excitation pulse, 3.84 ms refocusing pulse, and fat saturation pulse, 83 % SAR, (**b**) 2.56 ms excitation pulse, 3.84 ms refocusing pulse, and no fat saturation pulse, 70% SAR, (**c**) 3.84 ms excitation pulse, 2.56 ms refocusing pulse, and no fat saturation pulse, 90% SAR, and (**d**) 3.84 ms excitation pulse, 2.56 ms refocusing pulse, and fat saturation pulse, 100% SAR.

(a) 2.56 ms excitation pulse, 3.84 ms refocussing pulse and vendor-provided fat saturation (fat-sat) pulse, (b) 2.56 ms excitation pulse, 3.84 ms refocussing pulse and no fat-sat pulse, (c) 3.84 ms excitation pulse, 2.56 ms refocussing pulse and no fat-sat pulse, and (d) 3.84 ms excitation pulse, 2.56 ms refocussing pulse and product fat-sat pulse. In Fig. 4, SE EPI images were acquired with (a) 2.56 ms excitation pulse, 6.40 ms refocussing pulse and fat-sat pulse, (b) 2.56 ms excitation pulse, 6.40 ms refocussing pulse and no fat-sat pulse, (c) 6.40 ms excitation pulse, 2.56 ms refocussing pulse and no fat-sat pulse, and (d) 6.40 ms excitation pulse, 2.56 ms refocussing pulse and product fat-sat pulse. Figure 3b,c demonstrate clearly the scalp fat signal without the fat saturation pulse. It is shifted by 44 pixels or roughly 70%, as expected given the acquisition bandwidth and the 3.35 ppm chemical shift. Figure 3a,d show images when the fat-sat pulse is employed, in which the fat artefact is no longer visible. It is worth noting that the appearance of the artefact in Fig. 3b,c is quite similar, as one would expect from Eq. 5 as only the region of overlap between the fat slice excited and the fat slice refocussed will appear in the image.

Figure 4 shows images obtained from the sequences using our novel method, with longer RF pulse durations and correspondingly weaker slice-select gradients. Figure 4c,d demonstrate that an RF pulse as short as 6.40 ms is sufficient for achieving complete fat signal suppression, when the other RF pulse has 2.56 ms duration. Figure 4a,d confirm that adding the fat-sat pulse gives no further improvement. Comparison of the images in Figs. 3 and 4 shows that increasing the duration of either of the RF pulses within the given range does not affect the overall image quality. The total SAR is decreased most when the larger amplitude refocussing pulse is lengthened, as the legend of Fig. 4a,b demonstrate. Omission of the fat-sat pulse also gives a SAR reduction but at the expense of severe fat artifact, unless our method is also used (Figs. 3b,c and 4b,c). Finally, increasing the duration of the excitation pulse reduces SAR the least.

Figure 5 shows SE EPI images obtained from the second subject participating in the study, where the images were acquired at the position of the temporal lobes. They were obtained with the following parameters: (a) 2.56 ms excitation pulse, 3.84 ms refocussing pulse and fat-sat pulse provided by the vendor with optimal shim;

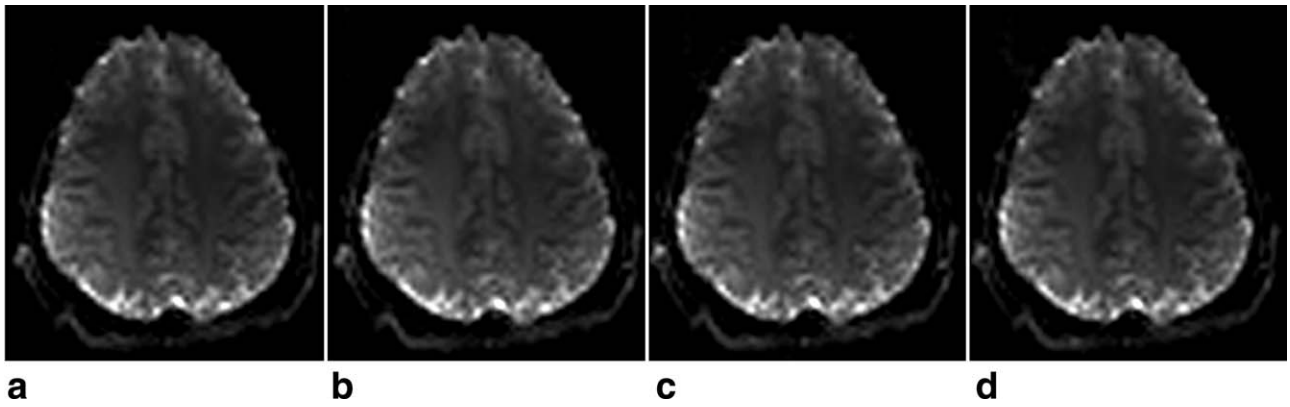

FIG. 4. SE EPI images acquired according to the proposed method with: (**a**) 2.56 ms excitation pulse, 6.40 ms refocusing pulse, and fat saturation pulse, 63% SAR, (**b**) 2.56 ms excitation pulse, 6.40 ms refocussing pulse and no fat saturation pulse, 50% SAR, (**c**) 6.40 ms excitation pulse, 2.56 ms refocusing pulse and no fat saturation pulse, 85% SAR, and (**d**) 6.40 ms excitation pulse, 2.56 ms refocusing pulse and fat saturation pulse, 95% SAR.

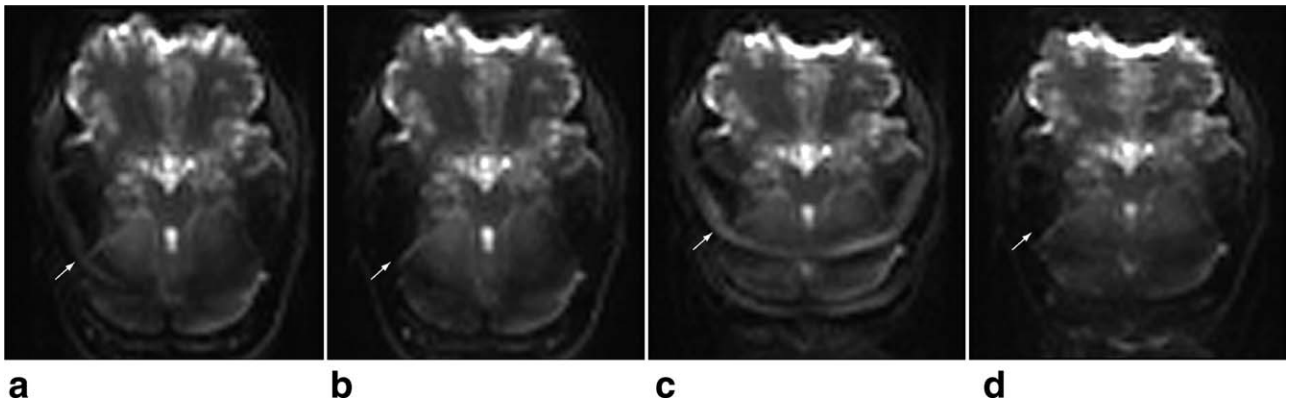

FIG. 5. SE EPI images acquired with: (**a**) 2.56 ms excitation pulse, 3.84 ms refocusing pulse and fat saturation pulse (conventional method) acquired under optimal shim conditions, (**b**) 2.56 ms excitation pulse, 6.40 ms refocusing pulse and no fat saturation pulse (proposed method) acquired under optimal shim conditions, (**c**) 2.56 ms excitation pulse, 3.84 ms refocusing pulse and fat saturation pulse (conventional method) acquired with mistuned shim, and (**d**) 2.56 ms excitation pulse, 6.40 ms refocusing pulse and no fat saturation pulse (proposed method) acquired with mistuned shim.

(b) 2.56 ms excitation pulse, 6.40 ms refocussing pulse and no fat-sat pulse with optimal shim; (c) 2.56 ms excitation pulse, 3.84 ms refocussing pulse and product fat-sat pulse with mistuned shim; and (d) 2.56 ms excitation pulse, 6.40 ms refocussing pulse and no fat-sat pulse with mistuned shim. Figure 5a demonstrates that fat saturation fails in areas of insufficient B_1 as indicated by the white arrow. In contrast, Fig. 5d indicates that the method proposed is more robust to B_0 inhomogeneities than fat saturation as the fat artefact to be seen in Fig. 5c is entirely suppressed.

Figure 6 shows a comparison across the whole brain between SE EPI images acquired with the fat saturation method, on the left-hand side of each column, and our proposed method on the right-hand side. In particular, the images on the left were acquired with 2.56 ms excitation pulse, 3.84 ms refocussing pulse and fat-sat pulse. The images on the right with 2.56 ms excitation pulse, 6.40 ms refocussing pulse and no fat-sat pulse. The images in Fig. 6 demonstrate that the water signal loss due to field inhomogeneities is quite comparable between the two methods, whereas the fat saturation fails to suppress the lipid signal in the inferior temporal regions, as indicated by the arrows.

The volumes acquired with 2- and 3-mm slice thicknesses using all sequence variants covered the whole brain, enabling estimation of the effects of slice-select gradient magnitude on image quality, both in well-shimmed areas and regions suffering from susceptibility gradients, which can give image drop-outs. When both slice-select gradients were in the same direction, the volumes obtained by averaging three slices with 1-mm thickness always showed a higher signal-to-noise ratio than the volumes acquired with 3-mm slice thickness. This is especially true for sequences with short RF pulse durations and strong slice-select gradients. The gain, resulting from reduced through-slice dephasing, is largest in areas affected by susceptibility gradients, and minor in those unaffected. By contrast, images obtained using the gradient reversal method have smaller overall signal-to-noise ratio when three 1-mm-thick slices are averaged, as compared with one 3-mm-thick slice, exacerbated by increasing difference in slice-select and refocussing gradient amplitudes. Here, inhomogeneity in B_0 causes an opposite bending of the slice between slice-excitation and refocussing, resulting in loss of signal.

Use of standard fat saturation pulses decreases the water signal in well-shimmed areas, due to magnetization transfer contrast effects and in regions of field inhomogeneities due to possible overlap of the fat-sat linewidth on to the water line.

DISCUSSION

We have shown that excellent fat suppression accompanied by a reduced SAR can be achieved by lengthening the refocusing pulse in a spin-echo EPI sequence. For the results presented in this study, a relatively low resolution was chosen. However, higher resolution can be achieved by employing partial Fourier acquisition and parallel imaging techniques (20,21).

Fat suppression can be achieved by lengthening either the excitation or refocussing pulse, the latter giving greater SAR reduction. However, this lengthens the minimum echo time. The choice depends on the application considered. For fMRI purposes, the increased echo time is still acceptable (22), and the smallest SAR is desirable for large volume coverage and extended time course runs. By contrast, for diffusion-weighted sequences lengthening the excitation pulse may be more desirable, to enable the shortest possible echo time and minimize loss of signal through T_2 decay. SAR is reduced both by omission of the fat-sat pulse and by reduction of either RF pulse amplitude. This immediately translates into an increased number of slices that can be acquired per TR. When the refocussing pulse is lengthened to 6.4 ms, as for example in Fig. 4b, the slice acquisition rate is doubled from five to 10 slices per second, when compared with the vendor's standard sequence in Fig. 3d, which has unsuitably short refocussing pulse for 7 T. Comparing the proposed method of Fig. 4b to the conventional method of Fig. 3a—a more convenient choice

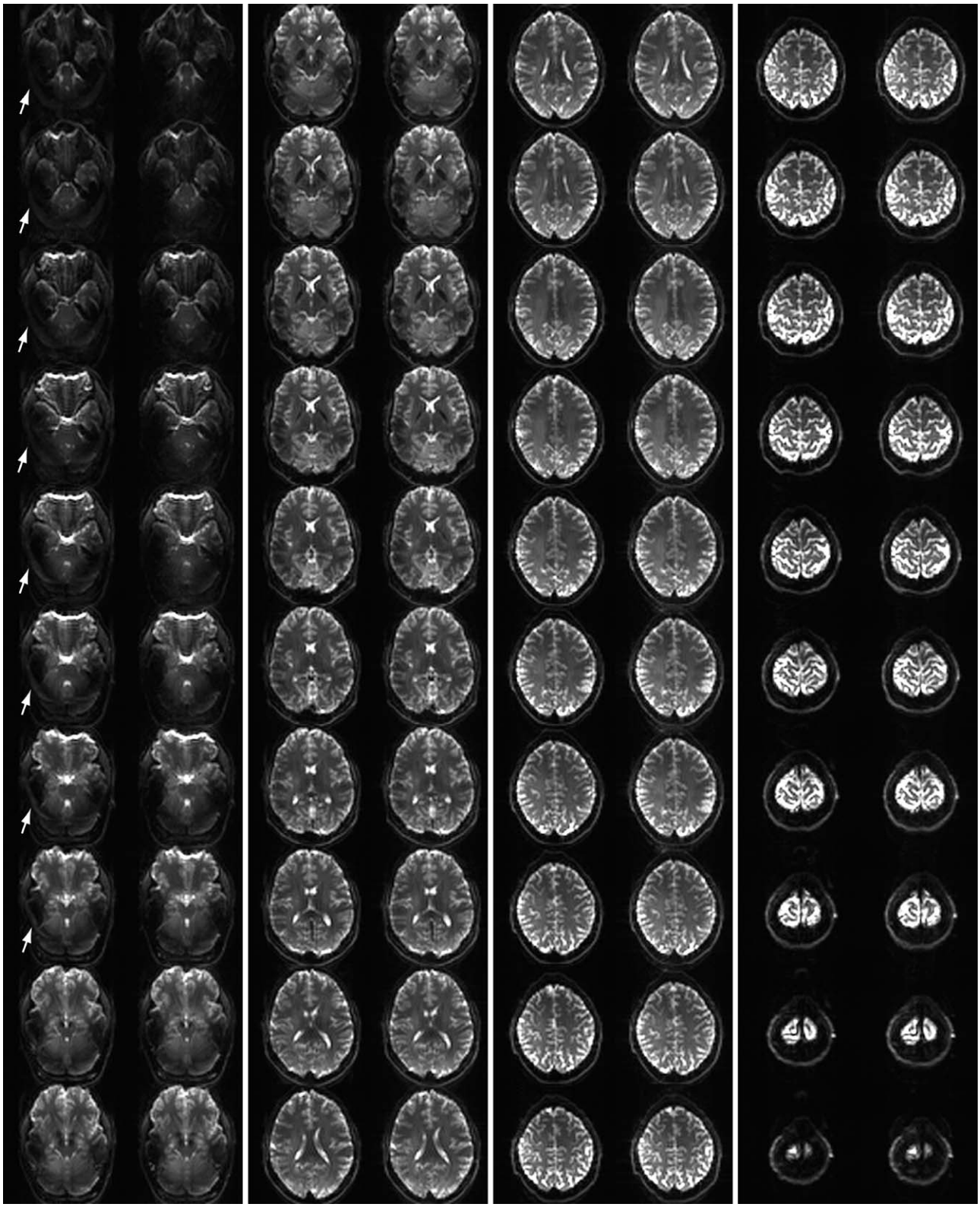

FIG. 6. Whole brain comparison between SE EPI images acquired with 2.56 ms excitation pulse, 3.84 ms refocusing pulse and fat saturation pulse (conventional method) on the left-hand side of the columns and 2.56 ms excitation pulse, 6.40 ms refocusing pulse and no fat saturation pulse (proposed method) on the right-hand side of the columns.

of pulse durations for reducing the power deposition—we still see a decrease in SAR of 40% (24% due to lengthening the refocusing pulse and 16% due to omission of the fat-saturation pulse). This decrease obtained can be utilized to increase the volume coverage by 65% for the same acquisition time, as can be calculated by taking the

ratio of the two SAR values (83% SAR/50% SAR). In comparison, if only the length of the refocusing pulse is increased and the fat-sat pulse is kept, the volume coverage gain is only 25% (63% SAR/50% SAR).

This method has been demonstrated using standard RF pulse shapes. Optimized pulse shapes, giving squarer slice profiles, would enable a smaller ratio between the durations of excitation and refocusing slice-select gradients for complete fat suppression. This is more critical at lower fields (such as 3 T), where using the standard RF pulse shapes would require one RF pulse to be more than five times longer than the other.

It should be mentioned that many other sequences, such as turbo spin-echo (23) and gradient-echo and spin-echo (24) can also employ the proposed fat suppression method. Methods using a fat-saturation pulse are extremely demanding for static magnetic field B_0 homogeneity, because such pulses do not suppress signal from off-resonance fat protons. They can also fail when there is too much B_1 inhomogeneity. If B_0 drifts over the long time courses typical of functional and diffusion scans, which have a high duty cycle and can thus heat passive shim material, the fat and the water signals both shift in frequency, making spectrally selective fat saturation less effective. The proposed method, however, is less sensitive to all of these problems. Even if the refocusing pulse is different from 180°, the crusher gradient following it ensures that any transverse fat magnetization generated by it is dephased. As the effect is less sensitive to magnetic field inhomogeneities than previous methods, it can be applied for imaging any body region.

There is one drawback of our method when very long RF pulses with correspondingly weak slice-select gradients are used. The resultant slice may be no longer flat but distorted in regions of severe field inhomogeneity. This can lead to a loss of the water signal in such regions, as the off-resonance water spins will not be refocused along with the fat spins. However, similar or even larger losses occur with the gradient reversal method with the same RF pulse durations, because here the slices excited and refocused will be distorted in opposite directions. With our method, such distortions have the same direction during excitation and refocusing, with smaller loss of water signal loss than with gradient reversal fat suppression.

It should also be mentioned that effective transverse relaxation time in brain at 7 T is generally long enough that no loss of water signal occurs during the longer RF pulse.

CONCLUSION

We have presented a novel fat-suppression method for spin-echo type sequences suitable for high magnetic field strengths. The proposed method is less sensitive to B_1- and B_0-field inhomogeneities than the standard frequency selective fat saturation method. It does not require additional RF and gradient pulses, and so it has a lower RF power deposition than other fat suppression methods which utilize these to eliminate the lipid signal. The decrease in SAR obtained by lengthening the refocusing RF pulse and eliminating the fat suppression pulses can be used to increase the volume coverage per unit time for SE EPI acquisitions, compared with conventional fat saturation techniques. In general, the method can be applied throughout the entire body. Although the method can be used at any field strength, it is especially important for high magnetic field strength, as demonstrated here at 7 T.

ACKNOWLEDGMENTS

Support by Siemens Healthcare Sector is gratefully acknowledged. The authors would like to thank Prof. Dr. Oliver Speck and Dr. Johannes M. Hoogduin for helpful discussions and Domenica Wilfling and Elisabeth Wladimirow for their assistance.

REFERENCES

1. Brown TR, Kincaid BM, Ugurbil K. NMR chemical shift imaging in three dimensions. Proc Natl Acad Sci USA 1982;79:3523–3526.
2. Pykett IL, Rosen BR. Nuclear magnetic resonance: in vivo proton chemical shift imaging. Radiology 1983;149:197–201.
3. Sepponen RE, Sipponen JT, Tanttu JI. A method for chemical shift imaging. J Comput Assist Tomogr 1984;8:585–587.
4. Dixon WT. Simple proton spectroscopic imaging. Radiology 1984; 153:189–194.
5. Ordridge RJ, Van de Vyver FL. Re: separate water and fat images MR images. Radiology 1985;157:551–552.
6. Glover GH, Schneider E. Three-point Dixon technique for true water/fat decomposition with B_0 inhomogeneity correction. Magn Reson Med 1991;18:371–383.
7. Bydder GM, Young IR. MR imaging: clinical use of the inversion recovery sequence. J Comput Assist Tomogr 1985;9:659–675.
8. Rosen BR, Wedeen VJ, Brady TJ. Selective saturation NMR imaging. J Comput Assist Tomogr 1984;8:813–818.
9. Haase A, Frahm J, Hanicke W, Matthaei D. 1H NMR chemical shift selective (CHESS) imaging. Phys Med Biol 1985;30:341–344.
10. Keller PJ, Hunter WW, Schmalbrock P. Multisection fat-water imaging with chemical shift selective presaturation. Radiology 1987;164:539–541.
11. Kaldoudi E, Williams SC, Barker GJ, Tofts PS. A chemical shift selective inversion recovery sequence for fat-suppressed MRI: theory and experimental validation. Magn Reson Imaging 1993;11:341–355.
12. Shin W, Gu H, Yang Y. Incidental magnetization transfer contrast by fat saturation preparation pulses in multislice Look-Locker echo planar imaging. Magn Reson Med 2009;62:520–526.
13. Park HW, Kim DJ, Cho ZH. Gradient reversal technique and its applications to chemical-shift-related NMR imaging. Magn Reson Med 1987;4:526–536.
14. Volk A, Tiffon B, Mispelter J, Lhoste JM. Chemical shift-specific slice selection. A new method for chemical shift imaging at high magnetic field. J Magn Reson 1987;71:168–174.
15. Gomori JM, Holland GA, Grossman RI, Gefter WB, Lenkinski RE. Fat suppression by section-select gradient reversal on spin-echo MR imaging. Radiology 1988;168:493–495.
16. Nagy Z, Weiskopf N. Efficient fat suppression by slice selection gradient reversal in twice-refocussed diffusion encoding. Magn Reson Med 2008;60:1256–1260.
17. Haacke EM, Brown RW, Thompson MR, Venkatesan R. Magnetic Resonance Imaging: Physical Principles and Sequence Design, 2nd ed. New York: Wiley-Liss; 1999. p 381–421.
18. Yacoub E, Duong TQ, Van De Moortele PF, Lindquist M, Adriany G, Kim SG, Ugurbil K, Hu X. Spin-echo fMRI in humans using high spatial resolutions and high magnetic fields. Magn Reson Med 2003;49:655–664.
19. Schäfer A, van der Zwaag W, Francis ST, Head KE, Gowland PA, Bowtell RW. High resolution SE-fMRI in humans at 3 and 7 T using a motor task. Magn Reson Mater Phys Biol Med 2008;21:113–120.
20. Griswold MA, Jakob PM, Heidemann RM, Nittka M, Jellus V, Wang JM, Kiefer B, Haase A. Generalized autocalibrating partially parallel acquisitions (GRAPPA). Magn Reson Med 2002;47:1202–1210.
21. Pruessmann KP, Weiger M, Schneidegger MB, Boesiger P. SENSE: sensitivity encoding for fast MRI. Magn Reson Med 1999;42:952–962.
22. Uludag K, Muller-Bierl B, Ugurbil K. An integrative model for neuronal activity-induced signal changes for gradient and spin echo functional imaging. Neuroimage 2009;48:150–165.
23. Hennig J, Nauerth A, Friedburg H. RARE imaging – a fast imaging method for clinical MR. Magn Reson Med 1986;3:823–833.
24. Oshio K, Feinberg DA. GRASE (GRAdient-echo and Spin-Echo) imaging – a novel fast MRI technique. Magn Reson Med 1991;20:344–349.